Theoretical aspects of the attenuation of pressure pulses within cerebrospinal-fluid pathways*

Miss P. Lockey **G. Poots**

Department of Applied Mathematics, University of Hull, England

Bernard Williams

Midland Centre for Neurosurgery & Neurology, Holly Lane, Smethwick, Warley, Worcs. B67 7JX, England

Abstract—*Coughing produces pulses of pressure in the cerebrospinal fluid. A mathematical model is proposed for the examination of the propagation of waves through the cerebrospinal-fluid pathways. The effects due to differing degrees of obstruction of the spinal-fluid pathway (blockage) on the attenuation factors and wave speeds are discussed as are the effects due to vibrations of the elastic dura.*

Keywords—*Cerebrospinal fluid, Modelling*

1 Introduction

THE TISSUES of the human central nervous system are bathed in a clear fluid which is a dilute solution of salts and protein. This cerebrospinal fluid (c.s.f.) is formed inside the ventricles which are within the brain and also lies outside the brain and the spinal cord in the subarachnoid space. It does not normally lie within the spinal cord, the only exception being in syringomyelia, a disease which is sometimes called hydromyelia. The transmission of energy through c.s.f. is responsible for several disease processes. The best known of these is hydrocephalus (water on the brain), which is principally a hydrostatic phenomenon, being due to the damming back of fluid formed within the ventricles. The c.s.f. is subject to pulsatile as well as hydrostatic pressures and pulsations probably play a part in hydrocephalus both alone and with spina bifida, as well as the principal part in the formation of syringomyelia, syringobulbia and various other cystic malformations.

The fluid in the spaces around the brain and spinal cord is bounded by two membranes, the arachnoid which is very thin and immediately outside that, the dura mater which is a fibrous membrane (Fig. 1). The subarachnoid space around the spinal cord approximates in shape to an annulus and in addition to c.s.f. contains nerves, vessels and fine supporting ligaments of the cord. In the skull, the dura is fastened to bone and is therefore rigid, but in the spine it demonstrates some elastic properties.

To gain some knowledge of the nature of propagation of pulse waves, a theoretical and practical study has been undertaken on the nature of the passage of cough impulses along the spinal canal.

*First received 16th February 1973 and in final form 22nd August 1974

2 Resting pressure of c.s.f.

Pressures within the c.s.f. pathways have traditionally been measured with the patient in a horizontal position lying on the side. An open-ended manometer has been connected to the subarachnoid space. Normally, fluid rises into the manometer and pressures are therefore given in millimetres of c.s.f. (virtually water) above the midline. Arterial blood pressures are higher and taken with a cuff connected to a mercury manometer. Mercury units are now commonly used for c.s.f. pressure recordings also. 1 mm Hg = 13·5 mm c.s.f. = 43·2 N/m².

The veins contain blood, the pressure in them

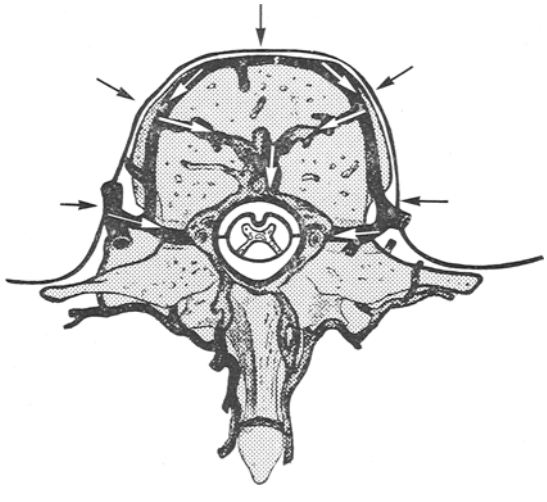

Fig. 1 Transverse section through the spine. The abdominal pressure (black arrows) is transmitted along the veins (white arrows) and is reflected in the c.s.f. which is represented as a clear, unshaded area around the cord

depends upon the position of the body and the state of muscular activity but is physiologically controlled so as to ensure the return of blood to the heart, even at rest. It is therefore usually approximately equal to atmospheric pressure at the upper end of the thorax when upright, or the midline when horizontal and on the side. Cerebrospinal-fluid pressure is usually about 10 mm Hg above venous pressure at rest.

3 Origin of cough impulses

Coughing produces a short sharp pressure rise within the major body cavities of the thorax and abdomen. The diaphragm is relaxed and the glottis closed, the intra-abdominal pressure is then raised by contraction of the trunk muscles and pressure is raised until the glottis relaxes, releasing air from the lungs whereafter the pressure drops to atmospheric and the cough is over (Fig. 2).

Coughs studied by WILLIAMS (1972) were those of the order of 0·9 s duration, pressure in the abdomen rises to around 75–100 mm Hg (Figs. 3 and 4).

4 Transmission of cough impulses to the spine

The spine is made up of vertebrae, a series of bones and tough ligaments which are enveloped by muscles. It forms part of the body wall which surrounds the abdominal and thoracic cavities. There is a spinal canal running through the bones and this is protected from the direct action of muscles. It is within the protection of this spinal canal that the spinal cord lies, surrounded by cerebrospinal fluid, arachnoid and dural membranes giving off a pair of nerves for each vertebra. Outside the dura there is a little fat and a plexus of epidural veins which lie chiefly on the front of the cord as two vertical channels which are crosslinked and supplied with anastomoses (connecting channels which allow flow in either direction) to the veins from bones of the spines, the veins within the surrounding muscles and to the veins of the abdominal cavities. The anastomotic veins occur at each segmental level. There are

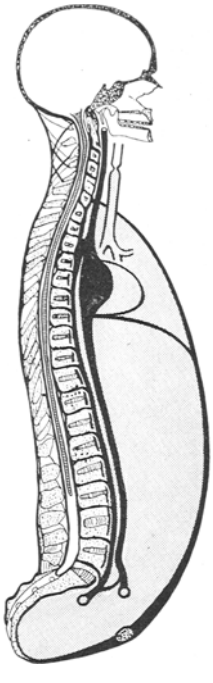

Fig. 2 Vertical section through the midline of the body. During coughing the area shaded in dots, up to the larynx, is subjected to sudden high pressure. This pressure is transmitted to the spinal canal whence it travels upwards. The veins are represented by the system of black lines connected to the heart and it can be seen that they are open to atmospheric pressure in the neck

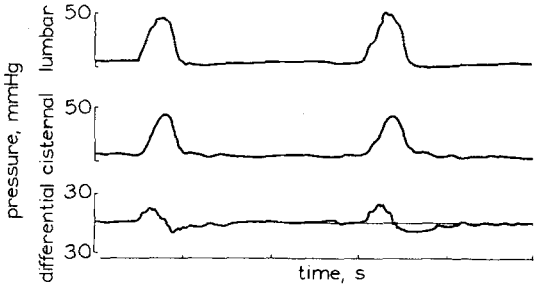

Fig. 3 Two normal coughs in the erect position. The manubrium is the top of the breast bone. The top trace is lumbar from the bottom of the spine. The middle trace is cisternal, from the base of the skull, the bottom trace is differential, lumbar minus cisternal. The mean attenuation factor is 91·5%. The pressure given is the pressure above the manubrium sterni

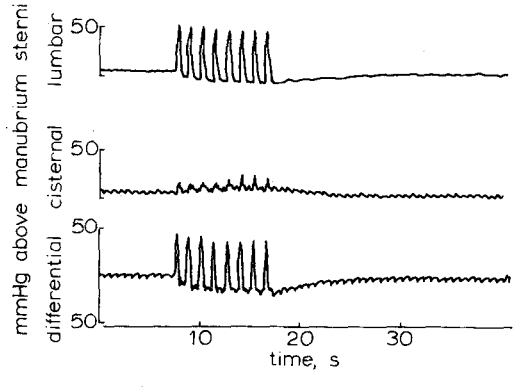

Fig. 4 Eight coughs in the presence of spinal block. Note the change in time scale from Fig. 3. The impulses are greatly attenuated by the time they reach the cistern. The mean attenuation factor is 23·5%

thirty vertebrae, each one corresponding to a segment throughout the spine. All but the topmost seven (cervical) vertebrae are intimately connected to the thoracic or abdominal cavities by veins (Fig. 2).

As the pressure in the thorax and abdomen rise during coughing, or any similar manoeuvre, the veins within the major body cavities are subjected to a high pressure and blood moves into the epidural veins transmitting most of that rise in pressure (Fig. 1). The increase in pressure is normally transmissible across the membranes forming the wall of the veins and across the dura and arachnoid to the c.s.f.

5 Recording c.s.f. pressure

Samples of pressure from human c.s.f. channels can be taken during routine clinical investigations from lumbar-puncture and cisternal-puncture needles. These are inserted between the vertebrae in the lumbar region and the cisterna magna, which can be reached between the skull and the highest cervical vertebra. These two sites are about 50 cm apart in adult subjects. Connection to recording apparatus allows a continuous record to be made. The method used by Williams is to record lumbar pressure as the top tracing, cisternal as the second tracing and the bottom tracing is a differential record lumbar minus cisternal pressure (Fig. 3). Williams has used the upright position because this is most relevant to human activity and in the belief that having the head high and therefore as a low-pressure zone, pulses will move upward more readily, although this assumption has not been tested.

6 Attenuation of cough impulse

Slow pressure changes are normally transmitted along the spinal canal with little attenuation. This has been known since 1830, when Queckenstedt described his test. The patient is positioned horizontally with a lumbar manometer in place. The neck is suddenly squeezed and the veins draining blood from the skull are thereby compressed, producing an increase in intracranial pressure. Normally, a rise occurs in the manometer-fluid level which falls when the neck is released. If there is a blockage affecting the spinal subarachnoid space between the skull and the lumbar puncture needle, then the rise in pressure in the lumbar region is absent or extremely slow. The rate of fall is also impaired in compressive lesions. Such impaired responses are therefore evidence of a compressive lesion of the spinal cord and the test is of value in the diagnosis of spinal paralyses. The accuracy of Queckenstedt's test has been improved by electrical recording apparatus (GILLAND, 1966; LAKKE, 1969) and also has been improved by recording from the cistern as well as the lumbar region so that the pressure change above the obstruction as well as below can be compared (AYER, 1921; GILLAND, 1966). Queckenstedt's test produces a movement of c.s.f. downwards initially followed by an upward rebound, but coughing produces a pulse in the opposite direction, that is it travels from the lumbar region to the cisternal.

The cough impulse provides a much sharper rise in pressure of higher amplitude and also provides a quick fall instead of a plateau effect.

It seemed that this was likely to be a much more sensitive test than Queckenstedt's for the detection of spinal block and also that a study of the cough impulse would provide a simple model for a preliminary analysis of the nature of cerebrospinal-fluid pulse-wave propagation.

The clinical results have been presented in brief elsewhere (WILLIAMS, 1972) and a more extensive report producing statistical correlations with clinical measurements of degrees of spinal block as determined by X rays is being prepared for publication.

7 Mathematical model

In proposing a preliminary mathematical model for the study of cerebrospinal-fluid pulse-wave propagation, as activated by a cough, severe restrictions must be made in the choice of the flow geometry and in the physics of the wave propagation.

The assumption is made that no significant wave propagation occurs in the veins outside the dura. The following flow configuration is then examined theoretically (Fig. 5). The cerebrospinal fluid is contained in an annulus, uniform in cross-section and of length l. It is bounded internally by the spinal cord assumed to have uniform circular cross-section of radius b. It is bounded externally by the elastic dura of thickness h and radius a ($>b$).

A block is simulated by thickening the cord radius to $b(1+\varepsilon)$ over a length l_2 and located a distance l_1 from the lumbar region. The distance from the block to the cisternal region is denoted by l_3 so that $l = l_1+l_2+l_3$. On varying the lengths l_1, l_2 and $b\varepsilon$, the effects of the size and location of the block can be investigated. When $\varepsilon = 0$ there is no blockage, and when $b(1+\varepsilon) = a$ complete blockage is achieved.

A difficult decision in the modelling arises in the choice of closure conditions to be employed at the lumbar and cisternal ends. The origin of the pressure pulse due to the cough is in the lumbar region, and, clearly, both the lumbar and cisternal regions have an ability to absorb and transmit energy. They also have a capacity to absorb a volume of c.s.f. with a corresponding change in pressure. This is a function of the compliance of the dura and the vessels around the c.s.f. spaces and its result in total is referred to as capacitance. The capacitance of the cisternal end is essentially that of the head and is normally greater than that at the lumbar end. From a mathematical viewpoint, it is simplest to look at extreme end conditions namely, if an end is 'closed' the fluid velocity is zero, and the capacitance zero; if 'open'

the excess pressure will be zero, and the capacitance infinite. The extreme conditions analysed are open or closed at the lumbar end and open at the cisternal. Closed cisternal conditions have also to be considered, and numerical results are presented for completeness. Only further experimental observations will indicate a more realistic modelling procedure for the capacitances of the lumbar and cisternal regions.

Alternatively, useful information can be obtained by examining the propagation of a plane wave coming from infinity to the vicinity of the block. Since the size of the block l_2 is small

$$\left(\frac{l_1}{l_2} \gg 1, \quad \frac{l_3}{l_2} \gg 1\right)$$

a limiting case is obtained depending only on a, b, ε and l_2 for $l_3 \to \infty$ and $l_1 \to \infty$.

With regard to the physics of the wave propagation, it is assumed (see LAMB, 1898) that the c.s.f. is an inviscid compressible fluid. Thus there is a simultaneous vibration in the c.s.f. as modified by the yielding of the dura, the longitudinal vibration of the dura as modified by the c.s.f. and the radial vibrations of the system. Owing to the inclusion of a block in the present flow geometry, it would be extremely difficult to include the effects due to a viscous c.s.f. [see, for example, the work of WOMERSLEY (1955) on the flow of blood in large arteries].

Consequently, a pressure wave in the c.s.f. is considered not to be damped by viscous forces but only attenuated by the presence of the block and the yielding of the dura. It is also assumed that excess pressures on propagation of the wave are small compared with the absolute pressure of the fluid. Moreover, all wave fronts are assumed to be plane and any distortions as they converge or diverge on the neighbourhood of the block are ignored.

Employing this mathematical model, it was proposed to examine standing waves with a view to obtaining at least some knowledge of

(*a*) speed of a pressure wave in the c.s.f. and the associated speed of the longitudinal dura wave; and

(*b*) attenuation of the pressure wave.

In Section 8, the effects due to the dura are ignored and the external boundary $r = a$ is taken to be rigid. Attenuation factors for a plane pressure wave propagation in a partially blocked annulus are then determined as a function of a, b, ε, l_1, l_2, l_3 and the specifications for the lumbar and cisternal regions. In Section 9, the effects due to an elastic dura are discussed. Finally, in Section 10 a discussion of the results is given.

8 Rigid-wall model

The governing equations for plane-wave propagation (see LANDAU and LIFSHITZ, 1959) are:

$$\frac{\partial^2 p}{\partial z^2} = \frac{1}{{c_0}^2}\frac{\partial^2 p}{\partial t^2} \quad . \quad . \quad . \quad . \quad . \quad . \quad . \quad . \quad (1)$$

and

$$\frac{\partial u}{\partial t} = -\frac{1}{\rho}\frac{\partial p}{\partial z} \quad . \quad . \quad . \quad . \quad . \quad . \quad . \quad . \quad (2)$$

where the wave speed $c_0 = \sqrt{\partial p/\partial \rho}$, p is the excess pressure, u the velocity of the c.s.f., ρ the density of the c.s.f., t the time, and z is measured from the lumbar end in the longitudinal direction along the axis of the annulus. Let the jth section, $j = 1$, 2 and 3, denote the three regions $0 \leqslant z \leqslant l_1$, $l_1 \leqslant z \leqslant l_1 + l_2$ and $l_2 \leqslant z \leqslant l_1 + l_2 + l_3$, respectively.

Consider the jth section of the annulus. There are two waves, one incident and one reflected. The excess pressure p_j is given by

$$p_j = ik\rho {c_0}^2 \{A_j \exp i(\omega t - kz) + B_j \exp i(\omega t + kz)\}, \quad (3)$$

representing waves travelling in the positive and negative z-directions with wave speed $c_0 = \omega/k$; ω is the pulsatance, $\omega/2\pi$ is the frequency and k is the wave number. Employing eqns. 2 and 3, the velocity of the c.s.f. is

$$u_j = \frac{k^2 {c_0}^2}{i\omega}\{-A_j \exp i(\omega t - kz) + B_j \exp i(\omega t + kz)\}$$

$$. \quad . \quad . \quad (4)$$

The unknown amplitudes A_j and B_j, for $j = 1$, 2, and 3, are now obtained for the specified conditions at the lumbar and cisternal regions, together with conditions of continuity in the pressure and volume rate of flow at the junctions of sections 1 and 2 and sections 2 and 3.

The open (lumbar)–open (cisternal) case

At the lumbar $z = 0$, $p_1 = 0$, yielding:

$$A_1 + B_1 = 0 \quad . \quad . \quad . \quad . \quad . \quad . \quad . \quad . \quad . \quad . \quad (5)$$

At $z = l_1$ there is continuity in pressure and volume rate of flow yielding:

$$A_1 + B_1 \exp 2ikl_1 = A_2 + B_2 \exp 2ikl_1 \quad . \quad (6)$$

and

$$-A_1 + B_1 \exp 2ikl_1 = \alpha(-A_2 + B_2 \exp 2ikl_1) \quad . \quad (7)$$

respectively. The ratio of the cross-sectional areas:

$$\alpha = \{a^2 - (1+\varepsilon)^2 b^2\}/(a^2 - b^2) \quad . \quad . \quad . \quad (8)$$

gives a measure of the degree of blockage.

At $z = l_1 + l_2$ continuity in pressure and volume rate of flow yields:

$$A_2 + B_2 \exp 2ik(l_1 + l_2) = A_3 + B_3 \exp 2ik(l_1 + l_2) \quad (9)$$

and

$$\alpha\{-A_2+B_2\exp 2ik(l_1+l_2)\}$$
$$=-A_3+B_3\exp 2ik(l_1+l_2) \quad . \quad . \quad . \quad . \quad . \quad (10)$$

respectively.

Finally, at the cisternal $z=l_1+l_2+l_3$, $u_3=0$, yielding

$$A_3+B_3\exp 2ikl=0 \quad . \quad . \quad . \quad . \quad . \quad . \quad (11)$$

Eqns. 5–11 are consistent, provided the wave number k is a root of the transcendental equation

$$\{(\alpha-1)-(\alpha+1)\exp 2ikl_3\}$$
$$\times\{(\alpha+1)\exp 2ik(l_1+l_2)+(1-\alpha)\exp 2ikl_2\}$$
$$-\{(\alpha+1)+(1-\alpha)\exp 2ikl_1\}$$
$$\times\{(\alpha-1)\exp 2ikl_3-(\alpha+1)\}=0 \quad . \quad . \quad . \quad . \quad (12)$$

The attenuation factor $|A_3/A_1|$ is determined from

$$\left|\frac{A_3}{A_1}\right|^2=\sin^2 kl_1(\cos^2 kl_2+\alpha^2\sin^2 kl_2)$$
$$+\frac{\cos^2 kl_1}{\alpha^2}(\alpha^2\cos^2 kl_2+\sin^2 kl_2)$$
$$+\frac{(1-\alpha^2)}{2\alpha}\sin 2kl_1\sin 2kl_2 \quad . \quad . \quad . \quad (13)$$

When the vessel is unblocked ($\alpha=1$, $\varepsilon=0$) the lowest root is

$$k=\pi/l \quad . \quad . \quad . \quad . \quad . \quad . \quad . \quad . \quad . \quad . \quad (14)$$

for a complete block $\alpha=0$ and

$$k=\pi/l_1 \quad . \quad . \quad . \quad . \quad . \quad . \quad . \quad . \quad . \quad . \quad (15)$$

For a partial blockage, the transcendental equation (eqn. 12) is readily solved using the Newton–Raphson procedure. Taking typical length scales for a human as $l=0{\cdot}5$ m, $b=5$ mm, $a=10$ mm, length of blockage $l_2=10$ mm and various $l_1=400$, 350 and 300 mm, the corresponding attenuation factors $|A_3/A_1|$ are given graphically in Fig. 6 for various ε ($0\leqslant\varepsilon\leqslant 1$).

The closed (lumbar)–open (cisternal) case

The analysis is exactly the same as for the open–open case except that eqn. 5 is replaced by

$$-A_1+B_1=0 \quad . \quad . \quad . \quad . \quad . \quad . \quad . \quad . \quad . \quad (16)$$

The corresponding transcendental equation for determining the wave number k is

$$\{(\alpha-1)+(\alpha+1)\exp(2ikl_1)\}$$
$$\times\{(\alpha-1)-(\alpha+1)\exp 2ikl_3\}\exp 2ikl_2$$
$$+\{(\alpha+1)+(\alpha-1)\exp 2ikl_1\}$$
$$\times\{(\alpha+1)+(\alpha-1)\exp 2ikl_3\}=0 \quad . \quad . \quad . \quad . \quad (17)$$

The attenuation factor $|A_3/A_1|$ is determined from

$$\left|\frac{A_3}{A_1}\right|^2=\cos^2 kl_1(\alpha^2\sin^2 kl_2+\cos^2 kl_2)$$
$$+\sin^2 kl_1(\alpha^2\cos^2 kl_2+\sin^2 kl_2)/\alpha^2$$
$$+\{(1-\alpha^2)\sin 2kl_1\sin 2kl_2\}2\alpha \quad . \quad . \quad (18)$$

When the tube is unblocked ($\alpha=1$) the lowest root for k is

$$k=\pi/2l \quad . \quad . \quad . \quad . \quad . \quad . \quad . \quad . \quad . \quad . \quad (19)$$

and for a complete block, k is given by eqn. 15. Typical values of the attenuation factor are given in Fig. 6 for various ε.

The limiting case of $l_1\to\infty$ and $l_3\to\infty$

Consider now the propagation of a plane pressure wave travelling from $z=-\infty$ in the direction of z increasing. It is necessary to find the characteristics of the transmitted wave after passage through the block at $z=l_1$. For convenience, choose a new origin $z=0$ at the block and let the length of the block be l_2 as before. For the sections $-\infty\leqslant z\leqslant 0$ ($j=1$) and $0\leqslant z\leqslant l_2$ ($j=2$), the wave representations are given by eqns. 3. and 4. For the transmitted wave in the section $l_2\leqslant z\leqslant\infty$ ($j=3$), the required expressions are:

$$p_3=ik\rho c_0^2 A_3\exp i(\omega t-kz) \quad . \quad . \quad . \quad . \quad (20)$$

and

$$u_3=-\frac{k^2 c_0^2}{i\omega}A_3\exp i(\omega t-kz) \quad . \quad . \quad . \quad (21)$$

Continuity in pressure and volume rate of flow at $z=0$ and l_2 yields the four relationships:

$$A_1+B_1=A_2+B_2 \quad . \quad . \quad . \quad . \quad . \quad . \quad . \quad . \quad (22)$$
$$-A_1+B_1=\alpha(-A_2+B_2) \quad . \quad . \quad . \quad . \quad . \quad (23)$$
$$A_2+B_2\exp 2ikl_2=A_3 \quad . \quad . \quad . \quad . \quad . \quad (24)$$
$$\alpha(-A_2+B_2\exp 2ikl_2)=-A_3 \quad . \quad . \quad . \quad (25)$$

These give, for any kl_2, the attenuation factor

$$\left|\frac{A_3}{A_1}\right|=4\alpha/\{(1+\alpha)^4+(1-\alpha)^4-2(1-\alpha^2)^2\cos 2kl_2\}^{\frac{1}{2}}$$
$$. \quad . \quad . \quad . \quad (26)$$

Minimum values of $|A_3/A_1|$ will occur for

$$\cos 2kl_2=-12\{(kl_2=(2n+1)\pi,\quad n=0,1,2,\ldots)\}$$

maximum values will occur when $\cos 2kl_2=+1$, $(kl_2=n\pi,\ n=1,2,3,\ldots)$.

Thus, for all α,

$$\max\left|\frac{A_3}{A_1}\right| = 1, \qquad \min\left|\frac{A_3}{A_1}\right| = \frac{2\alpha}{1+\alpha^2} \quad . \quad . \quad (27)$$

Consequently, for $0 \leqslant \alpha \leqslant 1$ and any kl_2, there exists the simple inequality:

$$\frac{2\alpha}{1+\alpha^2} \leqslant \left|\frac{A_3}{A_1}\right| \leqslant 1 \quad . \quad . \quad . \quad . \quad . \quad . \quad . \quad . \quad (28)$$

These minimum and maximum values are indicated in Fig. 6.

The analysis for the open-closed and closed-closed cases is not given, but computed results are included in Fig. 6.

The open-open case for a finite tube predicts the greatest reductions in the attenuation factor. For example, when $\varepsilon = 0{\cdot}95$, $l_1 = 400$ mm, a reduction of 16% is indicated; moreover, as l_1 decreases $|A_3/A_1|$ decreases until $l_1 = 350$ mm and then increases. The interpretation of these results in relation to clinical findings is given in Section 10.

In the above, the effect of the block is controlled by α and it is not necessary to state how the block is sited at $z = l_1$. Theoretically, it could be attached to the cord as shown in Fig. 5, but equally well it could be attached to the 'rigid' dura. The latter case is more common since the elastic dura is usually compressed from outside producing a constriction in the c.s.f. pathway.

It is of interest to examine theoretically the effects due to the vibrations of the elastic dura. So as to make this investigation mathematically tractable it is necessary to assume that the block is sited on the cord, as shown in Fig. 5.

9 Effects of the elastic dura

The following analysis follows closely the investigation of LAMB (1898) on the propagation of sound in a tube as affected by the elasticity of the walls. Lamb's work is modified to describe the present annular geometry with a partial block. An essential assumption of the analysis is that the wavelength is large, i.e. small wave number. In this context, it is meaningful to discuss the finite tube (see eqns. 14 and 15) but not the limiting case leading to maximum and minimum criterion (eqn. 27). In the latter, the wave lengths concerned are of the same order as the dura radius and consequently insurmountable mathematical difficulties would be incurred in the locality of the block.

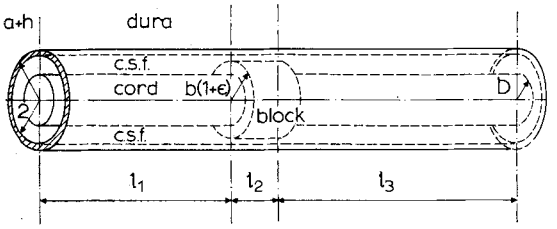

Fig. 5 Mathematical model of the c.s.f. pathway with block

Let ζ_j be the longitudinal displacement of the elastic dura and ξ_j denote its radial displacement. The corresponding extensions will be $\partial\zeta_j/\partial z$ along z, and ξ_j/a radially; $j = 1, 2$ and 3 is employed to denote the three sections. Let the density of the dura be ρ^* and in the usual notation E denotes Young's Modulus and σ is Poisson's Ratio.

The equations of motion for the dura ($j = 1, 2, 3$) are:

$$\frac{\partial^2\zeta_j}{\partial t^2} = \frac{B^*}{\rho^*}\left(\frac{\partial^2\zeta_j}{\partial z^2} + \frac{\sigma}{a}\frac{\partial\xi_j}{\partial z}\right) \quad . \quad . \quad . \quad . \quad (29)$$

$$\frac{\partial^2\xi_j}{\partial t^2} = \frac{p_j}{h\rho^*} - \frac{B^*}{\rho^*}\left(\frac{\xi_j}{a^2} + \frac{\sigma}{a}\frac{\partial\zeta_j}{\partial z}\right) \quad . \quad . \quad (30)$$

Here p_j is the excess pressure exerted by the c.s.f. on the dura; $B^* = E/(1-\sigma^2)$.

For the inviscid c.s.f., let w_j denote the longitudinal velocity and u_j the radial velocity. The pressure p_j is governed by the wave equation:

$$\frac{\partial^2 p_j}{\partial t^2} = {c_0}^2\left[\frac{1}{r}\frac{\partial}{\partial r}\left(r\frac{\partial p_j}{\partial r}\right) + \frac{\partial^2 p_j}{\partial z^2}\right] \quad . \quad . \quad (31)$$

where c_0 is the velocity of waves in an unlimited environment; $c_0 = \sqrt{\kappa/\rho}$ and κ is the cubical elasticity of the c.s.f. The velocity components u_j and w_j are given by Euler's equations:

$$\frac{\partial u_j}{\partial t} = -\frac{1}{\rho}\frac{\partial p_j}{\partial r} \quad \text{and} \quad \frac{\partial w_j}{\partial t} = -\frac{1}{\rho}\frac{\partial p_j}{\partial z} \; (j = 1, 2, 3)$$

$$. \quad . \quad . \quad . \quad (32)$$

Since the c.s.f. is inviscid, the following conditions must be applied. At the inner surface of the dura $r = a$:

$$u_j = \partial\xi_j/\partial t \quad . \quad . \quad . \quad . \quad . \quad . \quad . \quad . \quad . \quad . \quad (33)$$

and on the cord

$$u_j = 0 \text{ at } r = b_j\{b_1 = b_3 = b,\ b_2 = b(1+\varepsilon)\} \quad (34)$$

Consider now a plane pressure wave:

$$p_j = P_j(r)\{A_j \exp i(\omega t + kz) + B_j \exp i(\omega t - kz)\} \quad (35)$$

where $P_j(r)$ describes the variation in pressure with r; A_j and B_j are at present arbitrary constants. For the dura assume that:

$$\xi_j = D_j \exp i(\omega t + kz) + H_j \exp i(\omega t - kz) \quad (36)$$

and

$$\zeta_j = E_j \exp i(\omega t + kz) + J_j \exp i(\omega t - kz) \quad (37)$$

For eqn. 35, the wave equation (eqn. 31) reduces to

$$\frac{1}{r}\frac{d}{dr}\left(r\frac{dP_j}{dr}\right) - \nu^2 P_j = 0 \quad . \quad . \quad . \quad . \quad (38)$$

where

$$\nu^2 = k^2\left(1 - \frac{c^2}{{c_0}^2}\right) \quad . \quad . \quad . \quad . \quad . \quad . \quad . \quad (39)$$

The solution, in terms of zeroth-order modified Bessel functions, is

$$P_j(r) = F_j I_0(\nu r) + G_j K_0(\nu r) \quad . \quad . \quad . \quad . \quad (40)$$

where F_j and G_j are constants.

On insertion of eqns. 35 and 40, together with eqns. 36 and 37, into eqns. 32–34 and eqns. 29 and 30, and after some manipulation, there results the following:

$$p_j = \frac{k^2 c^2 \rho}{\nu}\left\{\frac{I_0(\nu r)\,K_0'(\nu b_j) - I_0'(\nu b_j)\,K_0(\nu r)}{I_0'(\nu a)\,K_0'(\nu b_j) - I_0'(\nu b_j)\,K_0'(\nu a)}\right\}$$

$$\times \{D_j \exp i(\omega t + kz) + H_j \exp i(\omega t - kz)\} \quad (41)$$

$$w_j = \frac{k^2 c^2}{\nu}\left\{\frac{I_0(\nu r)\,K_0'(\nu b_j) - I_0'(\nu b_j)\,K_0(\nu r)}{I_0'(\nu a)\,K_0'(\nu b_j) - I_0'(\nu b_j)\,K_0(\nu a)}\right\}$$

$$\times \{-D_j \exp i(\omega t + kz) + H_j \exp i(\omega t - kz)\} \quad (42)$$

the transcendental equation for the wave speed is

$$\left(c^2 - \frac{B^*}{\rho^*}\right)\left(c^2 + \frac{\rho N_j c^2}{h\rho^* k(1 - c^2/{c_0}^2)^{\frac{1}{2}}} - \frac{B^*}{\rho^* a^2 k^2}\right)$$

$$- \frac{\sigma^2}{k^2 a^2}\left(\frac{B^*}{\rho^*}\right)^2 = 0 \quad (43)$$

where

$$N_j = \frac{I_0(\nu a)\,K_0'(\nu b_j) - I_0'(\nu b_j)\,K_0(\nu a)}{I_0'(\nu a)\,K_0'(\nu b_j) - I_0'(\nu b_j)\,K_0'(\nu a)} \quad . \quad (44)$$

Eqn. 43 indicates that the wave speeds must alter in the locality of the block. This is not unreasonable, for it is known that the wave velocity is dependent on the effects of viscous damping. Considerable simplification is achieved on examining the limiting case of long wavelength, $k \to 0$. When $\nu \to 0$, eqn. 44 yields the limiting forms:

$$N_1 = N_3 \sim \frac{2a}{(a^2 - b^2)\,\nu} + 0(1) \quad . \quad . \quad . \quad (45)$$

and in the double limit $\varepsilon \to 0$, $\nu \to 0$

$$N_2 \sim \frac{2a}{(a^2 - b^2)\,\nu}\{1 + 0(\varepsilon^2)\} + 0(1) \quad . \quad . \quad (46)$$

Consequently, for small k and small ε the transcendental equation for the wave speed is

$$(c^2 - {c_0}^2)\left[(1 - \sigma^2)\frac{B^*}{\rho^*} - c^2\right]$$

$$= \frac{2a^3 \kappa c^2}{hB^*(a^2 - b^2)}\left(c^2 - \frac{B^*}{\rho^*}\right) \quad (47)$$

The constants D_j and H_j are now determined. At the junctions $z = l_1$ and $z = l_1 + l_2$ there is continuity in the volume rate of flow. However, it is necessary to assume continuity in the integrated pressures at these junctions as these cannot be matched exactly. The following conditions are invoked:

$$\left.\begin{aligned}
&\int_b^a w_1\, r\, dr = \int_{b(1+\varepsilon)}^a w_2\, r\, dr && \text{at } z = l_1\\
&\int_{b(1+\varepsilon)}^a w_2\, r\, dr = \int_b^a w_3\, r\, dr && \text{at } z = l_1 + l_2\\
&\int_{b(1+\varepsilon)}^a (p_1 - p_2)\, r\, dr = 0 && \text{at } z = l_1\\
&\int_{b(1+\varepsilon)}^a (p_3 - p_2)\, r\, dr = 0 && \text{at } z = l_1 + l_2
\end{aligned}\right\} \quad (48)$$

Insertion of eqns. 41 and 42 into eqns. 48 yields the following equations between the Dj and Hj:

$$-D_1 \exp 2ikl_1 + H_1 = -D_2 \exp 2ikl_1 + H_2 \quad . \quad (49)$$

$$-D_3 \exp 2ik(l_1 + l_2) + H_3 = -D_2 \exp 2ik(l_1 + l_2) + H_2 \quad (50)$$

$$\beta(D_1 \exp 2ikl_1 + H_1) = D_2 \exp 2ikl_1 + H_2 \quad . \quad (51)$$

$$\beta\{D_3 \exp 2ik(l_1 + l_2) + H_3\} = D_2 \exp 2ik(l_1 + l_2) + H_2 \quad (52)$$

where

$$\beta = 1 + \frac{b(1+\varepsilon)}{a} \times$$

$$\times \left(\frac{I_0'(vb)\,K_0'(vb_2) - K_0'(vb)\,I_0'(vb_2)}{I_0'(va)\,K_0'(vb) - I_0'(vb)\,K_0'(va)}\right) \quad (53)$$

For the open (lumbar)–open (cisternal) end conditions (cf. eqns. 5 and 11), the remaining relations are derived as:

$$D_1 + H_1 = 0 \quad . \quad . \quad . \quad . \quad . \quad . \quad . \quad . \quad (54)$$

and

$$D_3 \exp 2ikl + H_3 = 0 \quad . \quad . \quad . \quad . \quad . \quad . \quad . \quad (55)$$

Manipulation of eqns. 49–55 yields the same transcendental equation for k as given by eqn. 12 and the same expression for the attenuation factor $|H_3/H_1|$ as given by eqn. 13 provided α in eqns. 12 and 13 is replaced by β. Thus, within the framework of approximations already employed in deriving eqns. 45 and 46, it follows that as $\varepsilon \to 0$ and $k \to 0$

$$\beta \simeq \alpha\{1 + 0(\varepsilon^2)\} \quad . \quad . \quad . \quad . \quad . \quad . \quad . \quad . \quad (56)$$

The wave number and attenuation factors for the open-open case given in Fig. 6 are, for small blockage, unaltered by the vibrations of the dura. This conclusion is also true for the other finite-flow geometries but not, as previously mentioned, for the case yielding maximum and minimum limits of $|A_3/A_1|$.

Returning now to the calculation of the c.s.f. and dura wave speeds. For small k and small ε they are obtained on solving eqn. 47. Information on the elastic constants for living or dead dura are not available. The following physical properties were employed, namely:

$$E = 5 \times 10^8 \text{ N/m}^2, \quad \sigma = 0{\cdot}48, \quad \rho^* = 0{\cdot}95 \text{ g/cm}^3$$

For the c.s.f. values for water are employed, namely

$$\rho = 1 \text{ g/cm}^3 \text{ and } \kappa = 2{\cdot}22 \times 10^9 \text{ N/m}^2$$

Numerical solution of the approximate equation (eqn. 47) yields dura wave speeds of $1{\cdot}37 \times 10^3$, $4{\cdot}34 \times 10^3$, $1{\cdot}37 \times 10^4$ cm/s for dura thicknesses $h = 0{\cdot}01$, $0{\cdot}1$ and $1{\cdot}0$ mm, respectively. The acoustic

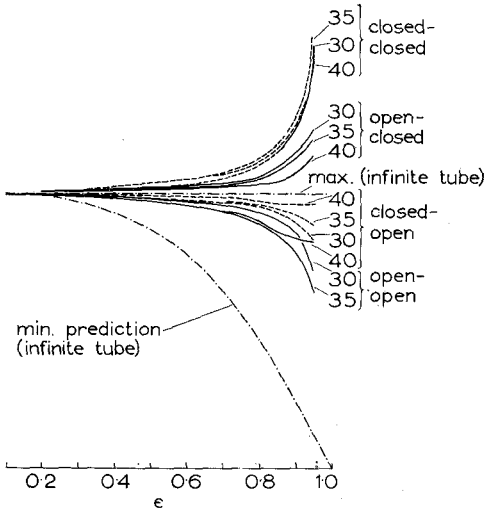

Fig. 6 Theoretical predictions of attenuation factors for various ε and block locations l_1 (see Fig. 5); $a = 10$ mm, $b = 5$ mm and $l_2 = 10$ mm, ... minimum and maximum criterion for the open or closed conditions

wave transmitted by the c.s.f. moves at a speed of $8{\cdot}27 \times 10^2$ m/s and is independent of the dura thickness. Consequently, the characteristics of this wave are unsuitable to clinical analysis.

On employing an iterative process involving eqn. 12, with α replaced by β, and taking N_2 in eqn. 43 the wave number k and wave speeds can be determined numerically for various h and ε. These are listed in Table 1 for $\varepsilon < 0{\cdot}5$. Note that the dura wave speed for fixed thickness decreases with increasing blockage; for fixed blockage it increases with increasing dura thickness.

Table 1. Theoretical predictions for dura wave speed as a function of the dura thickness and the size of the block

ε	h, mm	0·01	0·1	1·0
0		1·37	4·34	13·7
0·2		1·28	4·05	12·8
0·3		1·23	3·88	12·2
0·4		1·16	3·68	11·6
0·5		1·09	3·44	10·9

Dura wave speed (10 m/s); $a = 10$ mm., $b = 5$ mm., $l_1 = 400$ mm. $l_2 = 10$ mm., and $l_3 = 90$ mm. Wave speed for c.s.f. is $8{\cdot}27 \times 10^2$ m/s.

10 Discussion of results

In Fig. 6, attenuation factors for different sizes of blockages are displayed for finite-flow geometries and the limiting case of an infinite tube. The dura was assumed to form a rigid boundary. Clearly the open (lumbar)–open (cisternal) and closed (lumbar)–open (cisternal) configurations give a reduction in the attenuation factor with increasing size of blockage. The open-closed and closed-closed geometries yield increasing attenuation factors, with increasing size of blockage, and these results may have some bearing on the mechanisms of syringomyelia and syringobulbia.

In Section 9, the effects of the elastic dura, with a block sited on the cord, have been discussed. It is shown that the vibrations of the dura do not alter the size of attenuation factors for the finite tubes. The investigation does, however, yield information on the time taken for the pressure wave to travel from the lumbar to the cisternal region. From Table 1, it follows that over a length of 0·5 m of c.s.f. pathway the times taken were 0·04, 0·01 and 0·001 s for dura thickness $h = 0{\cdot}01$, $0{\cdot}1$ and $1{\cdot}0$ mm, respectively. From the observations of Williams (Fig. 3) on the pressure pulse, the time taken was of the order of 0·04 s. Thus the dura vibrations mainly control the times scales of the pressure-pulse propagation.

These theoretical predictions of the natural frequencies of the system cannot be compared directly to the clinical observations of Williams (1972). The effect of a cough is to produce a varia-

tion of the pressure $p = p(t)$ at the lumbar end, and the problem is to determine the propagation of this pressure variation along the c.s.f. pathway to the cisternal end. The duration of the pulse is far greater than the time for the wave to travel up and down the tube and the effect of this is that the natural frequencies, as discussed above, will probably appear simply as superpositions on top of the applied pulse; moreover, the natural frequencies will, in practice, have a lower amplitude than that of the pulse.

Further theoretical and experimental work is envisaged; for example, performing a spectral analysis of the experimental recordings of the cough pulse input so as to give the frequency components and appropriate amplitudes, it should then be possible to predict, on employing eqn. 13, the pressure pulse at the cisternal end for a specified degree of blockage. Comparing the latter for a range of ε with the observed cisternal output would then identify the degree of blockage.

Acknowledgment—One of the authors (P.L.) is indebted to the UK Science Research Council for a research studentship. The authors are indebted to G. A. Sargeant for Figs. 1 and 2.

References

AYER, J. B. (1921) Spinal subarachnoid block as determined by combined cisternal and lumbar puncture: with special reference to the early diagnosis of cord tumour. *Arch. Neurol. Psychiat. (Chic.)* **4,** 529–541.

GILLAND, O. (1966) *CSF dynamic diagnosis of spinal block.* Almquist & Wiksell, Stockholm.

LAKKE, J. P. W. F. (1969) Queckenstedt's test. *Exerpta. Med. Amsterdam.*

LAMB, H. (1898) On the velocity of sound in a tube, as affected by the elasticity of the walls. *Manchester Memoirs* **xlii,** 1–16.

LANDAU, L. D. and LIFSHITZ, E. M. (1959) In *Fluid Mechanics, Course of theoretical physics* **6.** Pergamon Press.

QUECKENSTEDT, H. H. G. (1916) Zur Diagnose der Ruckenmarkskompression. *Dtsch. Z. Nervenheilk* **55,** 325–333.

WILLIAMS, B. (1972) Combined cisternal and lumbar pressure recordings in the sitting position using differential manometry. *J. Neurol. Neurosurg. Psychiat.* **35,** 142–143.

WOMERSLEY, J. R. (1955) Oscillatory motion of a viscous liquid in a thin-walled elastic tube 1: the linear approximation. *Phil. Mag.* **46,** 199–221.

Aspects théoriques de l'affaiblissement des impulsions de pression dans les voies de passage du liquide cérébrospinal

Sommaire—La toux produit des impulsions de pression dans le liquide cérébrospinal. Cet article suggère un modèle mathématique pour l'examen de la propagation des ondes à travers les voies de passage du liquide cérébrospinal, et il examine les effets de différents degrés d'obstruction des voies de passage du liquide spinal (blocage) sur les facteurs d'affaiblissement et les vitesses de propagation des ondes, ainsi que les effets des vibrations sur la dura élastique.

Theoretische aspekte der dämpfung von druckimpulsen in den flüssigkeitskanälen von hirn und rückenmark

Zusammenfassung—Durch Husten werden Druckimpulse in der zerebrospinalen Flüssigkeit erzeugt. Zur Untersuchung der Fortpflanzung von Wellen durch die zerebrospinalen Flüssigkeitskanäle wird ein mathematisches Modell vorgeschlagen. Die auf die verschiedenen Behinderungsstärken für die Spinalflüssigkeitskanäle (Blockierungen) zurückzuführenden Auswirkungen auf die Dämpfungsfaktoren und Wellengeschwindigkeiten werden besprochen, ebenso die Auswirkungen von Schwingungen der elastischen Dura.